Targeted Cancer Therapy by Immunoconjugated Gold Nanoparticles *via* PEGylated Protein G

X.H. Sun, G.D. Zhang, D. Patel and A.M. Gobin*

*Department of Bioengineering, University of Louisville
Room 419, Lutz Hall, Univeristy of Louisville, KY 40292, USA
xinghsun@yahoo.com (XHS); andre.gobin@louisville.edu (AMG)

ABSTRACT

Targeted cancer therapy using near infrared (NIR) resonant immunoconjugated gold nanoparticles (GNPs) is promising photothermal therapeutics with regard to less invasive damage to the patient. To prepare a versatile immunoconjugated nanoparticle for targeting, PEGylated recombinant Protein G (PEG-ProG) was selected as a cofactor to immobilize immunoglobulins (IgGs) on GNPs by the F_c region, resulting in properly oriented IgGs. The bio-conjugated GNPs were characterized and showed good stability in physiologically relevant salt solutions. *In-vitro* studies showed that the ProG-PEG-conjugated GGS-NPs bound with anti erbB-2 (HER-2) IgGs successfully targeted HER-2 overexpressing breast cancer cells, SK-BR-3, and ablated them at low laser powers. As a control, low HER-2 overexpressing breast cancer cells, HTB-22, showed better survival at the same ablation conditions. Disruption of the cellular membrane due to localized hyperthermia was also observed.

Keywords: targeted cancer therapy, gold nanoparticle, Protein G, PEGylation, photothermal ablation

1 INTRODUCTION

Bio-conjugated metal or metal oxide nanoparticles (NPs) such as nanoshells, gold nanoparticles (GNPs) and iron oxide magnetic NPs have found increasing applications in biomedical engineering [1, 2]. GNPs with unique near infrared (NIR) resonance are excellent agents for early-stage diagnosis, and photothermal cancer cell ablation resulting from localized hyperthermia and disruption of the cell membrane or nucleus [3-5]. The optical characteristics are strongly related with a particle's size and geometry, such as silica-gold nanoshells, nanorods and nanocages [6-8]. The significance of the NIR region to medicine is due to the high transmission and low absorption of light from 650 nm up to 950 nm by native tissue components [3, 6, 9]. Gold-gold sulfide nanoparticles (GGS-NPs or GNPs) have been proven to be promising early-stage diagnostic and photothermal therapeutic agents [3, 10]. However, conjugating antibodies to the GNPs with their optimal activity toward the antigens is of importance to the active targeted imaging and therapy. Among the widely used strategies for bio-conjugation of GNPs: physical adsorption (by hydrophobic or electrostatic interaction), covalent immobilization, and specific binding using a cofactor [1, 2], immobilization of antibody on GNPs by F_c region via a cofactor can yield a versatile and highly efficient immunoconjugated NPs. IgG binding proteins like Protein A (ProA) and Protein G (ProG) are valuable candidates for such ordered antibody-immobilization.

Recombinant ProG is a small single-chain protein that is genetically expressed in *E. coli* and short of albumin-binding domains [11], which can be used to engineer a versatile bio-conjugated NP for antibody capture with maximal antigen-binding activity. ProG has a strong binding affinity to immunoglobulin G (IgG), especially to mouse IgGs. Binding the recombinant ProG that has no free-thiol groups to GNPs through physical adsorption leads to random coating and partial IgG-binding activity loss. More ordered immobilization of antibodies on GNPs were reported by pre-coating a genetically modified ProG with a cysteine tail to gold surfaces or more complex ProG-DNA conjugates [12, 13].

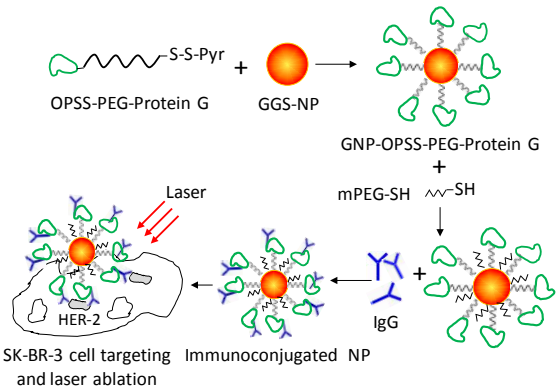

Figure 1: The schematic presentation of the targeted cancer therapy using the immunoconjugated GGS-NPs *via* PEGylated ProG.

In this work, we selected the PEGylated ProG (PEG-ProG) as a cofactor coated on GNPs to bind to antibodies for targeting therapy as shown in Figure 1. These GNPs with NIR absorption at around 860 nm were prepared and purified from a simple reaction between chloroauric acid and sodium thiosulfate that we have previously reported [14]. ProG was PEGylated with orthopyridyldisulfide-polyethylene-glycol-succinimidyl valerate (OPSS-PEG-SVA, average MW 2000). The PEG-ProG conjugated GNPs (ProG-PEG-GNPs) showed much better stability than the unconjugated GNPs in salt environments. The ProG-PEG-GNPs were then used to immobilize IgGs for

recognizing the antigens on the targeted cell membranes for further laser therapy. We propose that by using PEG-ProG as an IgG-binding cofactor, we can engineer a platform for the immobilization of various IgGs for targeted therapy of different cells. Rather than permanently attaching a specific antibody to the nanoparticle, it increases the versatility of the system. Two human breast cancer cell lines, SK-BR-3 cells that overexpress human epidermal growth factor receptor-2 (c-erbB-2 or HER-2), and HTB-22 cells with low HER-2 expression, were utilized as the positive target and negative control, respectively. SK-BR-3 cells were efficiently targeted and ablated by the as-prepared immunoconjugated GGS-NPs at the suitable conditions. Membrane damage caused by the ablation was also investigated by small florescent molecule, Lucifer Yellow (LY), and large molecule Texas Red labeled Dextran. Both are membrane-impermeable molecules to live cells.

2 MATERIALS AND METHODS

2.1 GGS-NP Synthesis and Characterization

GGS-NPs were synthesized by mixing 1.7 mM $HAuCl_4$ (Alfa Aesar) solution with 3 mM $Na_2S_2O_3$ solution at the volumetric ratio of 2.8 ($HAuCl_4$:$Na_2S_2O_3$). After 1 hr reaction, the as-synthesized GGS-NPs were then centrifuged (1200×g for 20 min) to remove most of the gold colloid by-products and increase purity of the NIR absorbing fraction of nanoparticles [10]. The pellets were collected and the corresponding supernatants were spun down again to increase yield. This process was repeated to obtain GGS NPs with minimal colloidal gold.

The NIR spectra of GNPs were characterized using a UV-Visible-IR spectrophotometer (Cary-50, Varian), and the size and zeta potential were measured using a Zetasizer (Nano-ZS90, Malvern). A FEI Tecnai F20 transmission electron microscope (TEM) operated at 200 kV was used to determine the shape and size of GNPs. The TEM samples were prepared by dropping 20 µl of aqueous gold particle suspension onto Holey carbon film enhanced TEM grids (C-flat^{TM}) followed by a room temperature drying.

2.2 PEGylation and Conjugation of Protein G on GGS-NPs

Recombinant ProG (Sigma-Aldrich) was PEGylated with OPSS-PEG-SVA (Laysan Bio) based on the modification of the method reported by Chattopadhyay *et al* [15]. Briefly, 0.5 ml of ProG (1 mg ml^{-1}) in pH 7.4 PBS was mixed with 0.5 ml of OPSS-PEG-SVA in 100 mM $NaHCO_3$ solution to achieve molar ratio of 1:10 or 1:25 (ProG:PEG) and was magnetically stirred for 3 hr at room temperature. The mixture was then stored overnight at 4 ºC. The products were purified to remove unreacted PEG using membrane ultrafiltration (MWCO 10 kDa, Pall). The purified PEGylated ProG was collected into 10 mM phosphate buffer, pH 7.4 and the concentration was assayed using Bradford reagent (Sigma-Aldrich). The conjugation efficiency was analyzed in a size exclusion column (SEC, Superose 12, GE Healthcare Bioscience) equipped in a Waters HPLC system. Samples were eluted using PBS consisting of 10 mM phosphate, 10 mM KCl and 140 mM NaCl at flow rate of 0.3 ml min^{-1}.

To conjugate the cofactor, PEG-ProG to GGS-NPs, the bare GNPs dispersed in DI water were first mixed with the PEG-ProG at a molar ratio of 500:1 (ProG:NP) for 1 hr at room temperature and continuing overnight at 4 ºC. Next, to block any remaining exposed gold surface, mPEG-SH (MW1000, Laysan Bio) was added to the ProG conjugated nanoparticles at a molar ratio of 500:1 (mPEG-SH:NP) overnight at 4 ºC. The ProG-conjugated NPs were then centrifuged twice at 2000×g for 20 min to remove the excess ProG and mPEG. Lastly, pellets were re-dispersed in PBS at a desired optical density.

To assess maximum antibody loading, IgGs captured by a ProG-conjugated GNP were quantitatively assayed by modifying the ELISA reported by Day *et al* [3] and the results were used to incubate anti-HER2 IgGs for laser ablation studies. Briefly, ProG-PEG-GNPs were first incubated with monoclonal mouse anti-HER-2 IgGs (Sigma-Aldrich) at a molar ratio of 200:1 (IgG:NP) for 20 min at room temperature and centrifuged twice to remove unbound IgGs. The GNP-PEG-ProG-anti HER-2 and control (mPEG-SH only) NPs were incubated with 100 µg ml^{-1} horseradish peroxidase (HRP)-conjugated goat anti-mouse IgGs (Sigma-Aldrich) in 3% of BSA in PBS (3% PBSA) for 1 hr at room temperature. The NPs were centrifuged twice to remove the excess HRP-conjugated anti-mouse IgGs and the pellets were re-suspended in 3% PBSA. The HRP-bound GNPs were developed using 3,3',5,5'-tetramethylbenzidine dihydrochloride (Sigma-Aldrich) with H_2O_2 for 15 min and the reaction was stopped by the addition of 2 M sulfuric acid. The count of anti-mouse IgG was calculated using a standard absorption curve of the appropriate HRP-conjugated anti-mouse IgG concentrations at 450 nm. The concentration of nanoparticles was calculated from the Beer-Lambert law with the extinction coefficient of GGS-NPs derived from Mie theory as described by Averitt *et al* [16].

2.3 Cell Culture and Laser Ablation

HER-2 overexpressing SK-BR-3 and control HTB-22 carcinoma cells were cultured in a 75 cm^2 (T-75) flasks using McCoy's 5A modified medium (ATCC) containing 10% fetal bovine serum (FBS) and 1% Penicillin-streptomycin-glutamine (PSG), and Minimum essential medium eagle containing 10% FBS, 1% PSG and 0.1% insulin, respectively. When cells were confluent, they were detached by Trypsin-EDTA (Mediatech). 50 µL of the cell suspension per well was then seeded with 1 ml cell media in a flat bottom 24-well microplate (Becton) to facilitate efficient laser irradiation by alternating plates thus subjecting cells to minimal disturbances in environment. Cells in wells were cultured at 5% CO_2 in an incubator for ~3 days prior to exposure to laser light.

When the cells were ~80% confluent, the cell media was removed and the cells were washed with PBS. A suspension of GNP-PEG-ProG (3.5 OD, ~6.8×10^{11} particles ml^{-1}) was incubated with anti-HER-2 antibody at a molar ratio of 60:1

(anti-HER-2:NP) for 20 min at room temperature. 0.5 ml of this immunoconjugated GNPs was then pipetted into each well. After incubation for 60 min, the cells were thoroughly washed with PBS. 0.3 ml of cell media was pipetted into each well and the cells were irradiated with an 817 nm laser (Coherent) using designed power by controlling power density and duration.

Cells were then incubated overnight and rinsed with PBS and tested for cell viability/cytotoxicity using a live/dead cell assay kit (Invitrogen). The stained cells were imaged with an Accu-scope 3032 fluorescence microscope (New York Microscope) equipped with a Nikon Sight DS-Qi/Mc digital camera (Nikon instruments). Images were analyzed using NIS-Elements AR 3.2 software (Nikon instruments). To investigate the SK-BR-3 cellular membrane damage resulting from hyperthermia due to GNPs under laser irradiation, the cell media was removed and the cells were rinsed with PBS. 0.5 ml of LY (Sigma-Aldrich) and Texas Red labeled Dextran (MW 10,000, Invitrogen) (both at 0.5 mg ml^{-1} concentration) was immediately added in the cells and incubated for 30 min at 37 ºC. After thoroughly washing with PBS, the cells were imaged using the fluorescence microscope. Green coloration shows LY while red shows Dextran.

3 RESULTS AND DISCUSSION

The SEC-HPLC chromatogram shows that the peak of the PEGylated ProG was shifted to the large molecule side (eluted earlier from the SEC), compared with the intact recombinant ProG (data are not shown). It indicates that the OPSS-PEGs were efficiently coupled to ProG by an amide bond, providing disulfide groups for the interaction with gold surfaces. Higher molar ratio of OPSS-PEG-SVA to ProG resulted in more PEG molecules attached per ProG molecule.

	Bare GNP	GNP-PEG-ProG	GNP-PEG-ProG-IgG
NIR absorption	858±14 nm	880±23 nm	883±26 nm
Diameter	46.8±4.0 nm	70.6±4.6 nm	89.3±6.7 nm
Zeta potential	-46.0±5.2 mV	-8.5±1.8 mV	-3.5±2.4 mV
IgGs captured	52.0±7.4 IgG/NP (PEG:ProG=25:1) 40.7±4.7 IgG/NP (PEG:ProG=10:1)		

Table 1: Characteristic parameter shifts and IgG capture efficiency by the PEG-ProG conjugated GNP. Bare and conjugated GNPs were suspended in DI water and PBS, respectively. Data were given in mean ± STD for n=4.

Table 1 shows the characteristic parameter changes during the conjugation, and the count of captured IgG of the PEG-ProG conjugated GNP using the ratios of OPSS-PEG-SVA to ProG at 10:1 and 25:1. Compared with the bare GNPs, the NIR absorption, hydrodynamic diameter and zeta potential of the bio-conjugated GNPs were all changed, indicating that the successful conjugation of the PEG-ProG on the GNP and the IgG-immobilization ability of the conjugated ProG. With the 2 KDa OPSS-PEG (Stokes diameter ~6.5 nm) [11,15] linked onto ~7 nm ProG, the ~25 nm increase in diameter demonstrated good attachment of PEG-ProG to GNPs [17, 18]. 52.0±7.4 IgG/NP for the PEG-ProG at PEG-SVA:ProG=25:1 showed better IgG-binding ability than the PEG-ProG at PEG-SVA:ProG=10:1, in which 40.7±4.7 IgG/NP was observed. As a control, 4.0±0.4 IgG/NP for mPEG-SH blocked particles was found. The molar ratio of OPSS-PEG-SVA to ProG was optimized to be 25 in this work.

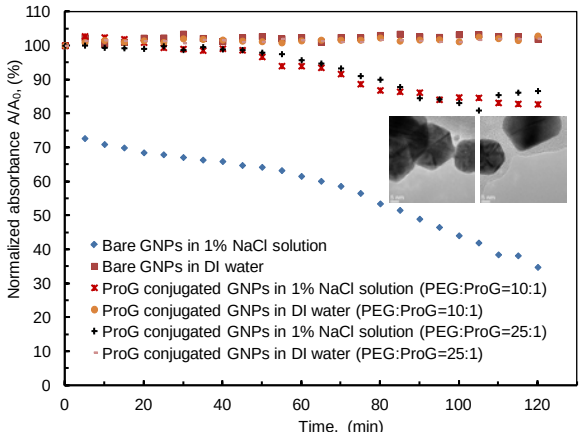

Figure 2: Stability of the PEG-ProG conjugated GNPs in 1% NaCl solution. Inset: TEM images of (left) bare GNPs and (right) PEG-ProG conjugated GNPs.

The stability of the conjugated GNPs in salt solution is another concern for therapeutic applications. As shown in Figure 2, the time-dependence change of the NIR absorption peak in 1% NaCl solution demonstrated the remarkable stability improvement for the PEG-ProG conjugated GNPs, compared with the bare GNPs. The inset TEM images also supported a nanoscale PEG-ProG layer coated around the GNPs that was related with the stable GNP-PEG-ProG.

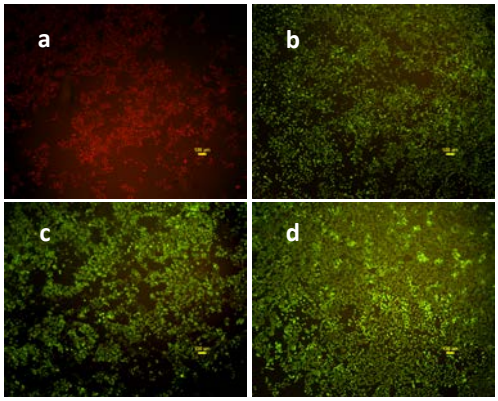

Figure 3: Live/dead stain images of SK-BR-3 (a-b) and HTB-22 (c-d) cancer cells incubated with GNP-PEG-ProG-anti HER-2 IgG after laser ablation with different operation conditions. (a, c) 3 W m^{-2} for 3 min (540 J). (b, d) 3 W m^{-2} for 2 min (360 J). Green stain shows dead cells and red shows dead ones.

The live/dead assay images as shown in Figure 3 after laser ablation indicated that 3 W cm^{-2} laser density at 3 min exposure (540 J power) effectively killed HER-2 overexpressing SK-BR-3 while lower power, 3 W / cm^{-2} for 2 min (360 J) showed poor ablation efficiency, and ProG only GNPs showed no cell ablation (Data not shown). As a control, HTB-22 cells with lower HER-2 expression was also treated at 540 J and showed high viability (Figure 3c).

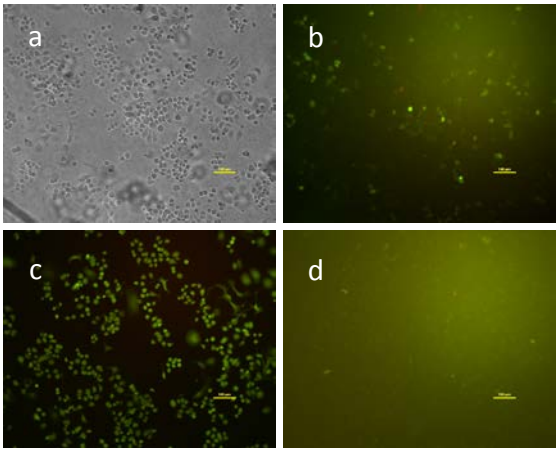

Figure 4: SK-BR-3 cellular membrane damage investigated using LY and Texas Red labeled Dextran after 3 W cm^{-2} laser ablation for 3 min (540 J) (a, b). (a) Bright field image of SK-BR-3; (b) Combined LY (green) and Dextran (red) fluorescent images; (c) Live/dead assay image of cells incubated with LY and Dextran with no laser irradiation; (d) Combined fluorescent images of cells incubated with LY (green) and Dextran (red) with no laser irradiation.

Figure 4 shows the LY and Texas Red labeled Dextran stain images of SK-BR-3 cells after laser irradiation. The damage to cell membrane integrity was seen using small molecule, LY as a tracer reagent. Compared with no laser treatment, the membrane damage at 540 J was significant. However, the large molecule, Dextran, was hard to diffuse through the damaged cellular membrane, indicating small holes induced by the local hyperthermia of the particles.

4 CONCLUSION

Immunoconjugation of GNPs using a protein cofactor is of importance to the preparation of a versatile GNP platform for improving the current targeted therapeutics. The presented successful bio-conjugation of the OPSS-PEG-ProG on the gold-gold sulfide nanoparticles (GGS-NPs) offers a practical protocol. *In vitro* studies showed that the ProG-PEG-conjugated GNPs bound with anti-erbB-2 (HER-2) IgGs were found to target HER-2 overexpressing breast cancer cell line, SK-BR-3 and showed almost total ablation at the selected laser power. The localized hyperthermia-induced damage to the cellular membrane integrity was also demonstrated using small florescent molecule. The unique near infrared (NIR) absorption of GNPs and the versatile antibody binding ability of the PEG-ProG demonstrated the proof-of-concept of photothermal cancer therapy using immunoconjugated GNPs *via* PEG-ProG.

ACKNOWLEDGEMENTS

This work was funded by the grant from Wallace Coulter Foundation: Early Career Phase I award, and NSF-EPSCoR No.0814194.

REFERENCES

[1] S. Rana, Y. C. Yeh, and V. M. Rotello, Curr. Opin. Chem. Biol., 14, 828-834, 2010.
[2] M. E. Aubin-Tam, and K. Hamad-Schifferli, Biomed. Mater., 3, 034001, 2008.
[3] E. S. Day, L. R. Bickford, J. H. Slater, N. S. Riggall, R. A. Drezek, and J. L. West, Int. J. Nanomed., 5, 445-454, 2010.
[4] L. R. Hirsch, A. M. Gobin, A. R. Lowery, F. Tam, R. A. Drezek, N. J. Halas, and J. L. West, Ann. Biomed. Eng., 34, 15-22, 2006.
[5] X. H. Huang, P. K. Jain, I. H. El-Sayed, and M. A. El-Sayed, Nanomedicine, 2, 681-693, 2007.
[6] A. M., Gobin, M. H. Lee, N. J. Halas, W. D. James, R. A. Drezek, and J. L. West, Nano Lett., 7, 1929-1934, 2007.
[7] X. H. Huang, S. Neretina, and M. A. El-Sayed, Adv. Mater., 21, 4880-4910, 2009.
[8] J. Y. Chen, B. Wiley, Z. Y. Li, D. Campbell, F. Saeki, H. Cang, L. Au, J. Lee, X. D. Li, and Y. N. Xia, Adv. Mater., 17, 2255-2261, 2005.
[9] R. Weissleder, Nat. Biotechnol., 19, 316-317, 2001.
[10] A. M. Gobin, E. M. Watkins, E. Quevedo, V. L. Colvin, and J. L. West, Small, 6, 745-752, 2010.
[11] B. Akerstrom, and L. Bjorck, J. Biol. Chem., 261, 240-247, 1986.
[12] J. M. Fowler, M. C. Stuart, and D. K. Y. Wong, Anal. Chem., 79, 350-354, 2007.
[13] Y. Jung, J. M. Lee, H. Jung, and B. H. Chung, Anal. Chem., 79, 6534-6541, 2007.
[14] G. D. Zhang, J. Jasinski, D. Patel, K. James, X. H. Sun, and A. M. Gobin, Proceedings of MRS 2011 fall meeting.
[15] N. Chattopadhyay, Z. L. Cai, J. P. Pignol, B. Keller, E. Lechtman, R. Bendayan, and R. M. Reilly, Mol. Pharm., 7, 2194-2206, 2010
[16] R. D. Averitt, S. L. Westcott, and N. J. Halas, J. Opt. Soc. Am. B-Opt. Phys., 16, 1824-1832, 1999.
[17] H. Jans, X. Liu, L. Austin, G. Maes, and Q. Huo, Anal. Chem., 81, 9425-9432, 2009.
[18] Y. L.Liu, M. K. Shipton, J. Ryan, E. D. Kaufman, S. Franzen, and D. L. Feldheim, Anal. Chem., 79, 2221-2229, 2007.